

Food & Function

Accepted Manuscript



This is an *Accepted Manuscript*, which has been through the Royal Society of Chemistry peer review process and has been accepted for publication.

Accepted Manuscripts are published online shortly after acceptance, before technical editing, formatting and proof reading. Using this free service, authors can make their results available to the community, in citable form, before we publish the edited article. We will replace this *Accepted Manuscript* with the edited and formatted *Advance Article* as soon as it is available.

You can find more information about *Accepted Manuscripts* in the [Information for Authors](#).

Please note that technical editing may introduce minor changes to the text and/or graphics, which may alter content. The journal's standard [Terms & Conditions](#) and the [Ethical guidelines](#) still apply. In no event shall the Royal Society of Chemistry be held responsible for any errors or omissions in this *Accepted Manuscript* or any consequences arising from the use of any information it contains.

1 **Structure and gelation properties of casein micelles doped with curcumin**
2 **under acidic conditions.**

3

4

5

6 Aya N. Khanji,^{a,b} Florentin Michaux,^a Jordane Jasniewski^a, Jeremy Petit^a, Emna Lahimer,^a,
7 Mohamed Cherif,^a Dominique Salameh^b, Toufic Rizk^b, Sylvie Banon^{a*}.

8

9 *corresponding author

10 tel : +33 (0) 383596073

11 fax : +33 (0) 383595772

12

13 ^a Université de Lorraine, Laboratoire d'Ingénierie des Biomolécules (LIBio), 2 avenue de la
14 Forêt de Haye, TSA40602-F-54518 Vandœuvre-lès-Nancy, France

15 ^b St Joseph University, Faculty of Sciences, UR TVA, Dept Chemistry, BP 11-514, Beirut
16 11072050, Lebanon.

17 **Highlights**

18 The positive values of enthalpy and entropy indicated that hydrophobic interactions were the
19 major binding forces governing curcumin and MC interactions.

20

21 The internal structure of micellar casein measured by SAXS did not vary upon curcumin
22 binding.

23

24 Curcumin did not produce any change of ζ -potential or size of micellar casein.

25

26 The ability of curcumin-doped micellar casein to produce acid gel was demonstrated.

27

28

29 **Abstract**

30 In this study, the ability of micellar casein (MC) to interact with curcumin during acidification
31 and to produce acid gel were investigated. Steady-state fluorescence spectroscopy of curcumin
32 variation and fluorescence quenching of caseins upon binding with curcumin molecules were
33 evidenced. Increasing the temperature from 20 to 35 °C enhanced MC-curcumin interactions as
34 reflected by the raise of binding constant from $0.6 \pm 0.3 \times 10^4$ to $6.6 \pm 0.6 \times 10^4 \text{ M}^{-1}$. From
35 changes in entropy, enthalpy and Gibbs free energy, hydrophobic interaction were proposed as
36 major binding forces. Static fluorescence MC quenching was demonstrated for MC-curcumin
37 complex during acidification. From pH 7.4 to pH 5.0, the binding sites number varied in the
38 range from 1.25 ± 0.05 to 1.49 ± 0.05 and the binding constant k_b varied from $3.9 \pm 0.4 \times 10^4$ to
39 $7.5 \pm 0.7 \times 10^4 \text{ M}^{-1}$. Small Angle X-Ray Scattering profiles demonstrated that MC internal
40 structure was unchanged upon curcumin binding. The ζ -potential value of curcumin-doped MC
41 indicated that curcumin did not modify the global charge of MC particles. Acid gelation studied
42 by oscillation rheology and static multiple light scattering at 20 and 35 °C led to similar
43 behavior for native and curcumin-doped MC suspensions. For the first time, it was demonstrated
44 that the colloidal and functional properties of MC were unchanged when doped with curcumin
45 during acidification.

46

47

48 Introduction

49 Micellar caseins (MC) in milk are considered as functional proteins for bringing digestible
50 protein to the neonate and preventing calcium phosphate precipitation in milk.^{1,2} Recent studies
51 also demonstrated that MC can carry bioactive molecules to tissue and cells³⁻⁵ MC consists in
52 colloidal particles of 100 nm radius built by interactions between about 10^4 casein molecules
53 and 800 nanoclusters of amorphous calcium phosphate.² Self-assembly of casein monomers
54 occurs through hydrophobic areas and calcium bridges between phosphoserine residues. The
55 internal structure of MC can be considered as a nano-gel⁶ and that contributes to its high
56 sorption and loading capacity of small molecules.^{7,8} Many bioactives are hydrophobic and thus
57 show poor aqueous solubility. In order to improve their dispersibility and bioavailability in
58 aqueous media, native or modified MC have already been used as delivery systems, as well as
59 α_s - and β -casein monomers, and their self-assemblies. For example, the various α_s - and β -
60 casein forms are avid binders of polyphenols.^{9,10}

61 Moreover, the acid-soluble calcium-phosphate bonds of MC and its sensitivity to proteolysis
62 provide an efficient release mechanism activated in the gastric and pancreatic stages of
63 digestion.³ MC presents also many advantages as labelled “Generally Recognized As Safe” food
64 proteins and highly stable materials during heat treatment and high-pressure processing.¹¹
65 Recent papers deal with the influence of food processing on curcumin binding with MC.
66 Curcumin is a natural polyphenol extracted from turmeric rhizome (*Curcuma longa*) that
67 presents a broad spectrum of biological activities including antioxidant, anti-inflammatory,
68 antimicrobial, antiamyloid and antitumor properties.¹² It presents a very low solubility in water
69 (2.99×10^{-8} M) at neutral or acid pH and becomes soluble in alkaline conditions albeit its very
70 high sensitive to hydrolysis. It was recently taken advantage of the pH-dependent solubility of

71 curcumin and the self-assembly properties of sodium caseinate in the pH range from 7 to 12 in
72 order to produce new MC delivery systems.¹³ Several studies have focused on curcumin/MC
73 interactions using the fluorescent properties of individual components.^{4,14} The binding constant
74 of curcumin with Ultra-High Pressure Homogenized MC (UHPH-MC) processed at 300 MPa
75 was significantly increased compared to native MC. This was explained by the dissociation of
76 MC into smaller micelles under high-pressure homogenization processing resulting in an
77 increase in their specific surface area available for interaction with curcumin.¹⁴ Static high-
78 pressure treatment of skim milk also enhanced the association of curcumin with MC, but the
79 mechanism proposed in the literature, related to structural modifications of MC (solubilization
80 of micellar calcium phosphate and MC size reduction), remains to be ascertained.¹⁵ Binding of
81 curcumin to MC was increased after milk heat treatment as a consequence of the formation of
82 heat-induced whey protein aggregates.¹⁶

83 To the best of our knowledge, only a few recent works deal with the influence of polyphenol
84 and curcumin on rennet-gelation of MC.^{17,18} Recently, it was shown that tea catechins
85 interacting with MC impacted both the primary and the secondary stage of milk rennet
86 aggregation¹⁸ but to our knowledge no study has been carried out on acid aggregation or
87 gelation. Milk acidification produces colloidal gel at around pH 4.6. Moreover, milk
88 acidification acts on MC stability by reducing the charge and inducing the solubilization of
89 micellar material (casein monomers at low temperature and minerals).^{19–22}

90 This study aimed at understanding the behavior of MC-curcumin complexes during
91 acidification. Direct steady-state fluorescence and tryptophan quenching were employed to
92 evaluate the extent of curcumin-MC interactions. The internal and overall structure of curcumin-
93 doped MC were analyzed by Small-angle X-ray scattering (SAXS) and Dynamic Light
94 Scattering (DLS). The influence of temperature and pH on the stability of MC-curcumin

95 complexes and their gelation properties were investigated by fluorescence spectroscopy, static
96 multiple light scattering and rheological measurements.

97

98 **Results and Discussion**

99 **Study of curcumin-MC interactions by fluorescence**

100 On the basis of interactions between the phenolic rings of curcumin and the hydrophobic amino
101 acid residues of tryptophan (trp) in caseins, curcumin binding to MC was studied through
102 fluorescence properties of both components (figures 1A and B). Fluorescence quenching at 344
103 nm indicated that MC tryptophan residues (1 to 2 trp residues per casein monomer) were
104 interacting with curcumin (figure 1C). Higher curcumin fluorescence at increased MC
105 concentrations indicated that curcumin molecules were transferred from the bulk to MC (figure
106 1D).

107 Quenching data was used to quantify curcumin-MC interaction from the modified Stern-Volmer
108 equation.²³

$$109 \quad \frac{F_0}{F_0 - F} = \frac{1}{fK_{SV} \cdot [\text{Cur}]} + \frac{1}{f} \quad (1)$$

110 where F_0 was the initial fluorescence intensity, F was the fluorescence intensity in the presence
111 of a quenching agent (such as curcumin), K_{SV} the Stern-Volmer quenching constant (M^{-1}), $[\text{Cur}]$
112 the curcumin (quencher) molar concentration (M), and f the fraction of accessible fluorophore to
113 a more polar quencher that permitted to determine the fractional fluorescence contribution of the
114 total emission for interaction with the studied quencher.²³ The Stern-Volmer quenching constant
115 K_{SV} was calculated from the plot of $F_0/(F_0 - F)$ vs. $1/[\text{Cur}]$ as the ratio between the y-axis
116 intercept ($1/f$) and the slope, $1/(f K_{SV})$.²³ At pH 7.4 and 6.5, K_{sv} were found at $18.2 \pm 0.2 \times 10^4$

117 and $18.8 \pm 0.9 \times 10^4 \text{ M}^{-1}$ respectively (table 1), which remained in the same order of magnitude
118 as literature values⁴, *i.e.* $11.3 \times 10^4 \text{ M}^{-1}$ (280 nm excitation and 342 nm emission) and 8.3×10^4
119 M^{-1} (295 nm excitation and 344 nm emission wavelength), or $7.2 \times 10^4 \text{ M}^{-1}$ (280 nm excitation
120 and from 300 to 450 nm emission).¹⁵

121 Concomitantly to the quenching of casein fluorescence by curcumin addition, a blue-shift of
122 tryptophan spectrum was noticed (figure 1A). The fluorescence of tryptophan is sensitive to the
123 polarity of its environment including hydration.¹⁴ The slight blue shift from 346.0 to 340.0 nm
124 was attributed to a more apolar tryptophan microenvironment through increasing curcumin
125 binding.^{14, 24} This effect was taken into account with the linearized form of the Stern-Volmer
126 equation that permitted to determine the number of binding sites (n) and the binding constant
127 (K_b):¹⁴

$$128 \quad \log_{10} \left[\frac{(F_0 - F)}{F} \right] = \log_{10} K_b + n \log_{10} ([Cur]) \quad (2)$$

129 The modeling of the current study led to an average n value of 1.47 ± 0.02 that was relevant
130 with the presence of one to two tryptophan residues per casein monomer in MC.² The binding
131 constant determined from quenching data (figure 1E) equaled $3.9 \pm 0.4 \times 10^4 \text{ M}^{-1}$ at pH 7.4 and
132 was in good agreement with literature values¹⁴ ranging from 2.4×10^4 to $5.6 \times 10^4 \text{ M}^{-1}$. This
133 binding constant range corresponds to non-covalent interactions.²⁵

134 From the spectral overlap of trp emission and curcumin absorption, dynamic quenching can
135 occur between the donor (trp) and the acceptor (curcumin). The quenching of donor (trp)
136 fluorescence can then be due to acceptor (curcumin) located at different distances and
137 orientations, and also to relative motions of donor and acceptor. All these contributions led to an
138 apparent decay of donor fluorescence that could be related to an apparent distance distribution
139 of acceptor. Considering very weak interactions between donor and acceptor, the evaluation of

140 distance between them can be evaluated from the Förster theory briefly described above and in
 141 details elsewhere.^{26, 27} On the basis of the Förster theory, the energy transfer efficiency, E , from
 142 the donor (trp) to the acceptor (curcumin) can be calculated from donor quenching:

$$143 \quad E = 1 - \frac{F}{F_0} \quad (3)$$

144 where F_0 and F , were the fluorescence intensity of tryptophan from MC in the absence and
 145 presence of curcumin, respectively.²⁶ The Förster critical distance, R_0 , at which 50% of the
 146 excitation energy was transferred from the donor to the acceptor can be calculated from equation
 147 (4) :

$$148 \quad R_0^6 = 8.785 \times 10^{-5} \frac{\kappa^2 \phi_D J}{n^4} \quad (4)$$

149 where κ^2 , the orientation factor between donor and acceptor, was chosen equaled to 2/3 for a
 150 random distribution. The quantum yield of donor in absence of acceptor, Φ_D , was fixed to 0.14
 151 as proposed for tryptophan in water between 300 and 450 nm.²⁶ The index of refraction, n , was
 152 taken to be 1.332 in PBS. J was the overlap integral between donor and acceptor and it was
 153 calculated from 300 to 450 nm according to:²⁶

$$154 \quad J = \sum_i F_D(\lambda_i) \varepsilon_A(\lambda_i) \lambda_i^4 / \sum_j F_D(\lambda_j) \quad (5)$$

155 where F_D was the normalized fluorescence spectrum of the donor, ε_A was the molar absorption
 156 coefficient of the acceptor. When ε_A and wavelength λ were expressed in $M^{-1} \cdot cm^{-1}$ and in nm,
 157 respectively, then J was expressed in units of $M^{-1} \cdot cm^{-1} \cdot nm^4$ and the Förster distance, R_0 ,
 158 calculated from equation (4) was in units of Å.²⁶

159 Once the energy transfer efficiency and the Förster distance were known, the average distance
 160 between donor and acceptor was calculated from:²⁷

$$E = \frac{R_0^6}{R_0^6 + r^6} \quad (6)$$

161 The Förster distance, R_0 , for MC and curcumin was found at 27 Å that falls into the usual range
 162 of R_0 values for tryptophan as donor, *i.e.* from 12 Å to 40 Å.²⁶ The average distance between
 163 MC and curcumin, r , was calculated at 33 Å. The distance r between pepsin and curcumin was
 164 recently found to be 24.5 Å within the curcumin-pepsin complex.²⁸ For curcumin and bovine- α -
 165 lactalbumin complex R_0 and r were found at 4-5 and 5-9 Å, respectively.²⁹ The overlap integral J
 166 and the energy transfer efficiency E were found at $1.6 \times 10^{-14} \text{ M}^{-1} \cdot \text{cm}^{-1} \cdot \text{nm}^4$ and 0.24
 167 respectively. As a comparison, E was found equaled to 0.13 for curcumin and bovine- α -
 168 lactalbumin complex.²⁹

170 Curcumin fluorescence was measured at a curcumin concentration of 5 μM , and increasing MC
 171 concentration. The binding constant was estimated by the equation of Wang and Edelman
 172 (1971):^{4,14, 30}

$$\frac{1}{\Delta F} = \frac{1}{\Delta F_{\max}} + \frac{1}{K_b \Delta F_{\max} [\text{MC}]} \quad (7)$$

174 where ΔF was the difference in fluorescence intensity at 500 nm between solutions with and
 175 without curcumin, ΔF_{\max} the maximum change in fluorescence, K_b the binding constant (M^{-1}) of
 176 curcumin with MC and $[\text{MC}]$ the casein micelle concentration expressed in molar unit. A
 177 binding constant K_b was calculated from the reverse plot of ΔF vs. $[\text{MC}]$, as the ratio between
 178 the y-axis intercept, $1/\Delta F_{\max}$, and the slope, $1/(\Delta F_{\max} \cdot K_b)$ (figure 1F). In this study, a K_b value of
 179 $0.6 \pm 0.1 \times 10^4 \text{ M}^{-1}$ was calculated by the double reciprocal method (cf. equation 7 and figure
 180 1F, $R^2 = 0.995$), which corroborated literature values obtained in similar conditions with $0.6 \pm$
 181 $0.3 \times 10^4 \text{ M}^{-1}$ and $1.5 \times 10^4 \text{ M}^{-1}$.^{4,14}

182 The ratios MC/curcumin ratios obtained at maximal quenching (figure 1C) and maximal
183 curcumin fluorescence intensities (figure 1D) were chosen to determine the influence of
184 curcumin addition on MC colloidal properties then on acid aggregation and gelation.

185

186 **Influence of temperature on curcumin-MC interactions**

187 Temperature was expected to influence curcumin-MC assemblies since hydrophobic interactions
188 between phenolic rings of curcumin and hydrophobic amino acid residues of caseins were
189 hypothesized. Moreover, it is well-known that the temperature range from 10 to 40 °C influence
190 the solubilization of hydrophobic β -casein and the voluminosity of MC.³¹ It was then relevant to
191 study curcumin-MC behavior over this temperature range by fluorescence.

192 From normalized fluorescence data of curcumin (at 5 μ M) as a function of MC concentration,
193 saturation curves (figure 2A) were obtained. Two behaviors were observed according to
194 temperature: the first one at 20 and 25 °C and the other one at 30, 35, and 40 °C. To reach half
195 of the maximal fluorescence intensity at 5 μ M curcumin concentration, twice the casein
196 concentration (12 μ M vs 6 μ M) was necessary at lower temperature (Figure 2 B). Increasing
197 temperature from 20 to 35 °C increased the binding constant K_b from 0.6 to $6.6 \times 10^4 \text{ M}^{-1}$ (Table
198 2). The obtained binding constants values were moderate and could be attributed to non-
199 covalent interactions. The increase in K_b values with temperature suggested that the binding
200 reaction between curcumin and MC was endothermic.²⁵ From K_b dependency to temperature,
201 the van't Hoff equation gave $\Delta H = +116.5 \pm 18.2 \text{ kJ.M}^{-1}$ and $\Delta S = +471.8 \pm 60.5 \text{ J.K}^{-1}.\text{M}^{-1}$. $\Delta H =$
202 $+114.5 \text{ kJ.M}^{-1}$ and $\Delta S = +471.8 \text{ J.K}^{-1}.\text{M}^{-1}$. This led to Gibbs free energy values, ΔG varying from
203 -21.7 to $-28.8 \text{ kJ.mol}^{-1}$ from 20 to 35 °C. The negative change in ΔG supported that curcumin
204 binding to MC was spontaneous. The positive values of enthalpy (ΔH) and entropy (ΔS)

205 indicated that hydrophobic interactions were the major binding forces governing interactions.²⁵
206 The positive value of enthalpy (ΔH) may be related to two main factors: the loss of hydrophobic
207 hydration structures when the curcumin molecules approached MC and the partial disintegration
208 of the bound water structure surrounding the curcumin molecules when they came into contact
209 with MC hydrophobic regions. The positive value of ΔS should be attributed to the release of
210 combined water molecules from protein or curcumin to buffer medium when curcumin bound to
211 MC. Another antioxidant molecule, α -tocopherol, showed the same thermodynamic profile for
212 enthalpy, entropy and Gibbs energy when interacting with human-serum albumin.²⁵ Another way
213 to enhance hydrophobic interactions of MC with curcumin was to remove β -casein from the
214 micellar system in order to increase the hydrophobic character of MC interior.³⁰ This resulted in
215 an increased binding of curcumin to modified-MC.³⁰ MC contains 20 000 casein monomers and
216 result from aggregation of α_s - and β - casein monomers with calcium phosphate then stabilized
217 with κ casein in surface.^{33,34} The open MC structures permit small molecules like curcumin to
218 enter and interact with α - or β -casein. In order to go further on the influence of curcumin
219 binding on MC structure, a multiscale characterization of the MC internal and overall structure
220 was performed. The influence of curcumin complexation on MC internal structure was studied
221 by SAXS. Moreover, MC size variation upon curcumin addition was investigated by DLS.

222

223 **Influence of curcumin on internal and overall MC structure in PBS buffer**

224 Small angle scattering methods allow the investigation of the size and shape of the entire casein
225 micelle or of its internal structure depending on the employed experimental q -range. The lower
226 the q -value, the broader the observation window of the system. Experiments performed by Ultra
227 Small Angle X-ray Scattering (USAXS) at low q -value of $3 \times 10^{-4} \text{ \AA}^{-1}$ were used to study the

228 entire casein micelle structure.³⁵ In this study, the experimental q -range (from 4×10^{-3} to 0.7 \AA^{-1}
229 ¹⁾ was suitable for investigating the variations of casein micellar internal structure upon
230 curcumin encapsulation. SAXS profiles of MC dispersion (superimposed and shifted in
231 intensity) are presented in **Error! Reference source not found.**3A and 3B. Samples without
232 curcumin have been analyzed at two sample-detector distances. The superimposition of the MC
233 patterns acquired at both distances (cf. circles and diamonds) confirmed the validity of the
234 mathematical treatment used to recover the absolute intensity in cm^{-1} . Mixtures of MC and
235 curcumin have been analyzed only using the long distance configuration.

236 The shape of the MC scattering curves was consistent with literature data about small-angle
237 scattering of casein micelles as reviewed recently.³⁶ At low angles ($4 \times 10^{-3} < q (\text{\AA}^{-1}) < 3 \times 10^{-2}$),
238 a near q^{-4} slope was detected corresponding to the form factor of the overall casein micelles
239 structure. An inflexion point was reported around 0.07 \AA^{-1} followed by a q^{-2} slope at high
240 angles. This signal was related to the form factor of calcium phosphate nanoclusters.^{5, 35} The
241 addition of different curcumin concentrations to the MC suspension did not show any influence
242 on the scattering profiles. All the curves were superimposed demonstrating that the internal
243 structure of the MC was not modified upon curcumin addition. Different results were reported
244 on the effect of tannins (epigallocatechin gallate, EGCG) addition on MC internal structure.⁵
245 EGCG addition to MC led to a higher scattered intensity at low angles due to an increase in the
246 global electronic density of the casein micelle. Moreover, the presence of tannins significantly
247 altered the scattering profile at high q values.⁵ Calcium chelation by EGCG resulted in the
248 disappearance of the inflexion at 0.07 \AA^{-1} .⁵ From our results, no sensible modification of the
249 scattering signal was observed upon curcumin addition to MC. This can be explained by the
250 difference in biomolecules concentration⁵; indeed, in the work of Shukla et al.⁵, EGCG
251 concentration was about thousand fold higher than the curcumin concentration of the current

252 study. More recently, Haratifar and Corredig found that up to 0.08 mg EGCG were bound per
253 mg of milk protein.¹⁸ No such high concentrations were tested with curcumin due to the fact that
254 curcumin concentration (5 - 50 μ M) was chosen with respect to the right biological activity
255 usually found for example against bone cancer cells over healthy bone cells or U2OS
256 osteosarcoma cells.^{37, 38}

257 DLS and ζ potential measurements were performed to acquire more information on size and
258 stability of MC doped with curcumin. The influence of raising temperature from 20 to 35 $^{\circ}$ C on
259 the size and charge of native and curcumin-doped MC was determined. The results obtained
260 after addition of curcumin did not reveal significant change in average MC size. At 20 $^{\circ}$ C, MC
261 size was determined at 187 ± 4 nm for control and 186 ± 3 nm after curcumin addition.
262 Increasing temperature up to 35 $^{\circ}$ C gave lower size at 175.8 ± 8.7 nm for control and 177 ± 8
263 nm after curcumin addition. Less hydration and lower voluminosity with higher temperature
264 explained such size variation.³⁹ The polydispersity index (PDI) was equaled to 0.16 ± 0.01 at 20
265 $^{\circ}$ C and 0.14 ± 0.01 at 35 $^{\circ}$ C for native and curcumin-doped MC respectively, indicating narrow
266 size distributions and no disturbance in overall MC structure. Either vitamin D₂ or
267 docosahexaenoic acid (DHA) could be incorporated into the hydrophobic core of re-formed MC
268 (from Na-caseinate supplemented with phosphate, citrate, and calcium ions) without variation of
269 MC size and morphology, as measured by dynamic light scattering and observed by TEM.¹¹
270 Small tannins were also carried by MC without change in its colloidal size.⁵

271 Curcumin addition to MC did not modify the overall charge and stability of MC. ζ potential
272 values equaled -12.0 ± 0.7 mV for MC control and -11.5 ± 1.2 mV for MC doped with
273 curcumin at 20 $^{\circ}$ C whereas -13.8 ± 0.7 mV and -14.1 ± 0.9 mV were respectively found at 35
274 $^{\circ}$ C.

275 X-ray and light scattering experiments revealed that the presence of curcumin did not modify
276 the MC internal and overall structure. These results suggested that MC can carry curcumin
277 without change in overall structure. The question then arises as to what the effect of loaded
278 curcumin on acid gelation properties of MC is. Further investigations of the current work were
279 focused on the influence of curcumin on MC colloidal stability under acidification in the 4.2 –
280 7.4 pH range between 20 and 35 °C. This was first studied by fluorescence spectroscopy.

281

282 **Influence of acidification on curcumin-MC interactions**

283 The quenching of trp fluorescence by curcumin binding to MC was observed after stabilization
284 of mixtures at pH values ranging from pH 5.0 to 7.4 (figure 4). It was demonstrated that MC
285 quenching by curcumin was stable during overall acidification and only a slight additional
286 quenching due to pH variation was noticed as for the control (MC without curcumin). This
287 slight MC quenching observed during acidification was probably due to more interactions
288 between amino acid residues in the tryptophan environment in relation with protonation,
289 demineralization and dehydration of MC. MC hydration (or voluminosity) decreased of about
290 30% from pH 6.6 to 4.8 while micellar calcium phosphate was fully solubilized.³²⁻³⁴ The pH-
291 dependent quenching variation influenced the binding constant K_b (equation 2) which increased
292 from pH 7.0 to 6.0 then decreased up to pH 5.0 while K_{SV} regularly increased with acidification
293 (Table 1). Then, K_b appeared more sensitive than K_{SV} to the quenching effect due to MC
294 acidification. The number of protein sites (n) was the second binding parameter calculated from
295 equation 2 and it was also found to be pH-dependent with values in the 1.25- 1.49 range (Table
296 2). At pH 7.4 in PBS, 1.47 binding sites were obtained for MC-curcumin complex, consistently
297 with the 1.20 binding sites found for curcumin interacting with bovine- α -lactalbumin.²⁹

298 κ_q , the bimolecular quenching rate constant, was calculated from K_{SV} according to $K_{SV} = \kappa_q \times \tau_0$
299 where τ_0 is the average lifetime of the biomolecule. For a biomolecule without a quencher, τ_0 can
300 be estimated at 10^{-9} s.²⁹ Then, in the pH range from 7.4 to 5.0, κ_q varied from 1.8×10^{14} to $3.2 \times$
301 10^{14} $M^{-1} s^{-1}$ which is higher than the limiting diffusion constants of the biomolecules upon
302 interaction with various quenchers ($\kappa_q = 2 \times 10^{10}$ $L \cdot mol^{-1} \cdot s^{-1}$).²⁹ Then, according to κ_q
303 fluorescence, quenching arose mainly from static mechanism by complex formation in the
304 ground state.²⁹

305

306 **Influence of curcumin addition on the sol-gel transition measured by multiple static light** 307 **scattering and rheological measurements**

308 The sol-gel transition of MC samples acidified with GDL was followed by the evolution of the
309 relative back scattered intensity (ΔBS) all along the sample height every 5 min after GDL
310 addition. One result concerning MC-curcumin sample at 35 °C is presented in Figure 5-A for
311 instance. From the time of GDL addition, an increase in ΔBS was reported corresponding to MC
312 aggregation as the intensity of scattered light increased with particle size and concentration.³²
313 This increase occurred all along the sample height, meaning that aggregation was homogeneous.
314 No syneresis was evidenced, as the evolution was independent from sample height. The
315 temporal evolution of the ΔBS average (calculated between 15 and 45 mm sample height) is
316 presented in Figure 5-B in relation with the elastic modulus G' profile that illustrated gel
317 formation. ΔBS rapidly varied with acidification indicating that particle aggregation began much
318 sooner than gelation ((classically considered to occur when G' becomes greater than 1Pa).⁴⁰
319 Acid gelation followed by ΔBS and G' profiles was compared for MC controls and MC doped
320 with curcumin at 20 and 35 °C (Figure 6). The addition of curcumin did not affect gelation

321 occurring around pH 4.4 and 4.6 at 20 and 35 °C respectively. Three steps were identified from
322 Δ BS variation with pH at 20 and 35 °C: a first slight variation from the initial pH to around pH
323 5.2 when MC are demineralized, then a rapid increase was obtained from pH 5.2 down to pH 4.8
324 that might be related to an increase in particle size that is more pronounced at 35 °C than at 20
325 °C. Finally, a plateau value was reached whereas the sol-gel transition occurred when
326 aggregates interacted to form a colloidal gel.

327 In this study, higher binding constants were obtained at 35 °C compared to 20 °C indicating
328 more interactions between curcumin and MC with temperature. Increasing hydrophobic
329 interactions were proposed as the major contribution to the raise in binding constants. With
330 acidification below the isoelectric pH of caseins, enhancement of hydrophobic interactions was
331 expected as a consequence from protein charge neutralization and lower hydration of MC³³
332 whereas curcumin stays in neutral form (indeed, its pK_a values were reported at pH 8.38 ± 0.04,
333 9.88 ± 0.02 and 10.51 ± 0.01).⁴¹

334 It was recently observed that curcumin and resveratrol increased the delay of rennet gelation.¹⁷
335 ¹⁸ Chelating calcium with polyphenols was proposed to inhibit rennet gelation by decreasing
336 calcium binding with caseins. The partial covering of MC with curcumin was also proposed to
337 compete with casein-casein interactions.¹⁸ During acidification, it was not evidenced any effect
338 of curcumin addition on MC gelation. The number of protein sites available for interaction with
339 curcumin (n) was found from 1.25 to 1.49. This low value should explained the preservation of
340 the main colloidal properties of MC, *i.e.* size, structure and charge. This indicated that curcumin
341 and certainly other hydrophobic biomolecules should be conveyed efficiently by MC in the
342 moderate acid conditions of yogurt-like products.

343

344 **Material and methods**

345 **Material**

346 The native-like phosphocaseins micelles (MC) used in this study were prepared by milk
347 microfiltration and diafiltration using milk ultrafiltrate (Promilk 872 B, Ingredia Dairy
348 Ingredients, Arras, France)), prior to stabilization in powder form by spray-drying. It contained
349 95% (w/w) dry solids and, on a dry weight basis, 87% total proteins (about 80%
350 phosphocaseins), 7.3% minerals, 5% lactose, and 0.8% fat. Bovine serum albumin (BSA),
351 curcumin, glucono-delta-lactone, and sodium azide were purchased from Sigma-Aldrich (Saint-
352 Quentin Fallavier, France). All other chemicals, of analytical grade, were provided by Carlo
353 Erba (Milan, Italy).

354

355 **Preparation of solutions**

356 Stock solutions of curcumin ($\geq 94\%$ purity) were prepared in ethanol (96%) at 1.0 mg.mL^{-1} and
357 stored protected from light at $4 \text{ }^\circ\text{C}$. Different curcumin concentrations were obtained from the
358 stock solution by dilution in ethanol just before use. Phosphate Buffered Saline (PBS) solution
359 (adjusted to pH 7.4 with HCl) was prepared with ultrapure water and contained for one liter: 8 g
360 NaCl, 0.2 g KCl, 1.44 g Na_2HPO_4 , 0.24 g KH_2PO_4 . In order to prevent bacterial growth, sodium
361 azide (0.02% (w/v)) was added to PBS buffer. PBS buffer filtration through $0.2 \text{ }\mu\text{m}$
362 polyethersulfone membrane (Millipore) was performed before use. MC were dispersed in PBS
363 buffer (pH 7.4) and stirred overnight at room temperature ($20 \text{ }^\circ\text{C}$) in order to get maximal
364 protein hydration and stabilization. MC concentration was determined by Lowry-Folin assay
365 using BSA as reference protein.⁴ In the whole document, MC molar concentrations were always
366 expressed in equivalent BSA concentrations. On a dry weight basis, 1 g.L^{-1} MC was equivalent

367 to 16.7 μ M BSA. Curcumin and MC mixtures were prepared in order to not exceed 2% (v/v)
368 addition of ethanol and thus avoiding protein denaturation. Controls were made with MC
369 suspensions containing ethanol without curcumin at a level not exceeding 2% (v/v) of ethanol.
370 Unless indicated, curcumin and MC mixtures were stirred for 1 h at room temperature before
371 use. The influence of acidification on curcumin-MC interactions was investigated by hydrolysis
372 of various amounts of Glucono-delta-lactone (GDL) in both kinetic and steady-state conditions.
373 Acidification was monitored with the Lab 850 pH-meter (SCHOTT® Instruments, Germany).
374 Each experiment was triplicated.

375

376 **Fluorescence spectroscopy**

377 The study of curcumin - MC interactions was carried out with a FLX spectrofluorimeter (Safas,
378 Monaco), which was temperature-controlled from 20 to 35 °C (\pm 0.5 °C) by circulating water.
379 Curcumin fluorescence was measured at 5 μ M in the presence of MC concentrations varying
380 from 0 to 55.8 μ M. The emission spectra were recorded from 450 to 700 nm with an excitation
381 wavelength of 420 nm. The slit widths used for curcumin fluorescence were 2.5 and 5 nm for
382 excitation and emission, respectively. MC suspensions without curcumin were used as controls.
383 MC quenching was determined at 8.9 μ M for various curcumin concentrations ranging from 0 to
384 40 μ M. The emission spectra were recorded from 300 to 450 nm at an excitation wavelength of
385 280 nm. Slit widths were 10 and 2.5 nm for excitation and emission respectively. Curcumin
386 solutions free from MC were used as controls.

387 Curcumin solutions and MC suspensions were vigorously mixed during 30 s in a 5 mL-tube,
388 then transferred into quartz cuvette (1 cm path length) for analysis. Each experiment was
389 performed in triplicate.

390

391 Size measurements by Dynamic Light Scattering

392 The hydrodynamic diameter of MC was measured by Dynamic Light Scattering using the
393 Zetasizer Nano-ZS (Malvern Instruments, Malvern, UK). The apparatus was equipped with a
394 532 nm frequency doubled DPSS laser He/Ne type. Particle size distributions were determined
395 using a low volume disposable cuvette (Zen0112, Malvern Instruments, UK). CONTIN analysis
396 model at 173° detecting angle was applied to transform the autocorrelation function into particle
397 size distributions. Data were assessed by Zetasizer software 7.10 (Malvern Instruments). PBS
398 buffer (1.332 refractive index and 0.86 mPa.s viscosity at 25 °C) was chosen as dispersant. MC
399 and curcumin concentrations were fixed at 15.8 µM and 51.0 µM respectively in order to get a
400 MC: curcumin ratio that corresponds to around 80% MC quenching (figure 1C). Absorption and
401 real refractive indexes of protein were 0.001 and 1.450, respectively. A delay of 300 s between
402 size measurements was to ensure sample equilibration at desired temperature.

403

404 ζ-potential measurements

405 The zeta potential is an indirect measure of the surface charge, which is an indicator of the
406 colloidal stability of particles. This was determined using a dynamic light scattering instrument
407 (Zetasizer Nano ZS, Malvern Instruments, Malvern, UK) fitted with a high concentration sample
408 cell. The high concentration cell enabled the measurement of the MC zeta potential with no dilution
409 of PBS buffer that was chosen as MC dispersant. MC concentration was fixed at 15.8 µM and
410 curcumin at 51.0 µM. Each experiment was made in triplicate.

411

412 Small Angle X-Ray Scattering

413 SAXS measurements were carried out at SOLEIL synchrotron at the SWING beamline (12 keV
414 energy). Two distances between sample and CCD camera, 1.47 and 2.97 m, were used to cover
415 q -ranges from 8×10^{-3} to 0.7 \AA^{-1} and 4×10^{-3} to 0.4 \AA^{-1} respectively, where $q = 4\pi \sin(\theta)/\lambda$ is
416 the modulus of the scattering vector, 2θ is the scattering angle, and λ is the X-ray wavelength.
417 The q -range calibration was achieved with a silver behenate standard ($d_{\text{ref}} = 58.38 \text{ \AA}$). For the
418 absolute intensity calibration, scattering patterns of the empty capillary and the capillary filled
419 with deionized water were first recorded. The value of the constant intensity contribution of
420 water is equal to 0.016 cm^{-1} on the absolute scale. Then, the signal of the same capillary filled
421 with the solvent solution was recorded for subtraction purposes before the introduction of the
422 studied samples.

423

424 **Multiple light scattering measurements for milk gelation**

425 The aggregation of MC dispersions after GDL addition (3% (w/v)) was followed by multiple
426 light scattering measurements using a Turbiscan Classic MA2000 apparatus (Formulation,
427 France) using a pulsed near-infrared light source ($\lambda = 850 \text{ nm}$). Addition of ethanol in the
428 mixtures of MC and curcumin (1 mg.mL^{-1}) did not exceed 2% (v/v). The low solubility of
429 curcumin in ethanol (1 mg.mL^{-1}) implied limited addition of curcumin to high concentration of
430 MC. The final concentrations for MC and curcumin equaled 501 and 51 μM respectively and
431 this corresponded to the ratio MC/ curcumin found in figure 1D for the maximal soluble
432 curcumin concentration. Two synchronous detectors measured transmitted and backscattered
433 light upon sample height by several scans all along a glass cylindrical cell from the bottom to
434 the top of the sample (5 - 7 cm analysis height) by incremental movements of 40 μm . In the
435 case of MC dispersions, only the backscattered light intensity (at 135° from the incident beam)

436 has been followed upon sample height since no transmitted light was detected. Backscattered
437 intensities all along the sample have then been performed upon time. One scan has been
438 recorded every 5 minutes after GDL addition (t_0). The first scan recorded at t_0 has been
439 subtracted from the following scans in order to highlight the system evolution upon time using
440 Turbisoft software. Then, the relative percentage of backscattered intensity (ΔBS) upon sample
441 height was reported. The evolution of the average backscattered intensity upon time has also
442 been plotted using this software. An increase of ΔBS upon time all along the sample height
443 corresponds to a homogenous aggregation of the particles. If an increase is detected at the
444 bottom of the glass cell and a decrease is reported at the top, a sedimentation occurs. An
445 evolution on the opposite way corresponds to a creaming of the dispersion. Measurements have
446 been performed in triplicates. The entire Turbiscan device has been placed in an oven to perform
447 the measurements at 35 °C. Turbiscan measurements began 3 min after GDL addition and
448 stirring.

449

450 **Viscoelastic measurements of acid milk gelation**

451 The curcumin and MC mixtures were prepared as indicated in the previous section. GDL (3%
452 (w/v)) was gently stirred in MC (501 μM) and curcumin (51 μM) mixtures for 3 min and a 20
453 mL aliquot was immediately transferred into the gap of coaxial cylinders (DIN C25) of the
454 Kinexus rheometer (Malvern Instruments, UK). The sol-gel transition and the development of
455 the gel structure was followed using 0.1% shear strain and 1.0 Hz frequency at controlled
456 temperatures 20 and 35 °C. The time at which the storage modulus (G') became greater than 1
457 Pa was considered as the gelation point. Each test was performed in duplicate.

458

459 Conclusion

460 Curcumin interaction with MC was confirmed by fluorescence spectroscopy. From binding
461 constant calculation, it was shown that higher temperature favored curcumin - MC interactions,
462 as expected for hydrophobic molecules. X-ray and dynamic light scattering experiments
463 revealed that curcumin did not modify MC internal and overall structures. MC ζ -potential
464 remained unchanged after curcumin addition. Hence, MC can load curcumin without change in
465 their overall structure and charge. The slight variation in binding constants in the pH range from
466 7.4 to 5.0 indicated that curcumin should be conveyed efficiently by MC in these moderate acid
467 conditions. The acid milk gelation was not disturbed after curcumin addition at 20 and 35 °C.
468 Further investigations should be necessary to understand the dependence of curcumin release by
469 MC on temperature and pH variations. This would allow improving the controlled-delivery from
470 MC during gastric and pancreatic digestion phases in order to favor curcumin and other
471 polyphenols bioavailability in dairy foods.

472

473 Acknowledgements

474 Authors would like to thank Marie-José Stébé and Marianne Impéror for their help during
475 SAXS experiments. This study was supported by grants from Erasmus Mundus (Program
476 Element), Region Lorraine and Université de Lorraine (Program CPER 5, Nutralor). All of these
477 are gratefully acknowledged.

478 **References**

479

- 480 1 C. Holt, N. M. Wahlgren and T. Drakenberg, *Biochem. J.*, 1996, **314**, 1035–1039.
- 481 2 C. Holt, *Curr. Opin. Struct. Biol.*, 2013, **23**, 420–425.
- 482 3 Y. D. Livney, *Curr. Opin. Colloid Interface Sci.*, 2010, **15**, 73–83.
- 483 4 A. Sahu, N. Kasoju and U. Bora, *Biomacromolecules*, 2008, **9**, 2905–2912.
- 484 5 A. Shukla, T. Narayanan and D. Zanchi, *Soft Matter*, 2009, **5**, 2884–2888.
- 485 6 C. G. (Kees) de Kruif, S. G. Anema, C. Zhu, P. Havea and C. Coker, *Food Hydrocoll.*,
486 2015, **44**, 372–379.
- 487 7 H. M. Farrell Jr., E. L. Malin, E. M. Brown and P. X. Qi, *Curr. Opin. Colloid Interface*
488 *Sci.*, 2006, **11**, 135–147.
- 489 8 D. S. Horne, *Curr. Opin. Colloid Interface Sci.*, 2002, **7**, 456–461.
- 490 9 E. Jöbstl, J. R. Howse, J. P. A. Fairclough and M. P. Williamson, *J. Agric. Food Chem.*,
491 2006, **54**, 4077–4081.
- 492 10 I. Hasni, P. Bourassa, S. Hamdani, G. Samson, R. Carpentier and H.-A. Tajmir-Riahi,
493 *Food Chem.*, 2011, **126**, 630–639.
- 494 11 E. K. Efrat Semo, *Food Hydrocoll.*, 2007, 936–942.
- 495 12 B. Joe, M. Vijaykumar and B. R. Lokesh, *Crit. Rev. Food Sci. Nutr.*, 2004, **44**, 97–111.
- 496 13 K. Pan, Y. Luo, Y. Gan, S. J. Baek and Q. Zhong, *Soft Matter*, 2014, **10**, 6820–6830.
- 497 14 A. Benzaria, M. Maresca, N. Taieb and E. Dumay, *Food Chem.*, 2013, **138**, 2327–2337.
- 498 15 S. Rahimi Yazdi, F. Bonomi, S. Iametti, M. Miriani, A. Brutti and M. Corredig, *J. Dairy*
499 *Res.*, 2013, **80**, 152–158.
- 500 16 S. Rahimi Yazdi and M. Corredig, *Food Chem.*, 2012, **132**, 1143–1149.
- 501 17 S. Haratifar and M. Corredig, *Food Chem.*, 2014, **143**, 27–32.
- 502 18 D. S. Horne, *J. Colloid Interface Sci.*, 1986, **111**, 250–260.
- 503 19 D. G. Dalgleish and A. J. R. Law, *J. Dairy Res.*, 1989, **56**, 727–735.
- 504 20 S. Banon and J. Hardy, *J. Dairy Sci.*, 1992, **75**, 935–941.
- 505 21 J. A. Lucey, M. Tamehana, H. Singh and P. A. Munro, *J. Dairy Res.*, 1998, **65**, 555–567.
- 506 22 P. Bourassa, J. Bariyanga and H. A. Tajmir-Riahi, *J. Phys. Chem. B*, 2013, **117**, 1287–
507 1295.
- 508 23 D. Z. Liu, M. G. Weeks, D. E. Dunstan and G. J. O. Martin, *Food Chem.*, 2013, **141**,
509 4081–4086.
- 510 24 J. T. Vivian and P. R. Callis, *Biophys. J.*, 2001, **80**, 2093–2109.
- 511 25 X. Li, D. Chen, G. Wang and Y. Lu, *Eur. J. Med. Chem.*, 2013, **70** 22–36.
- 512 26 P. Wu and L. Brand L., *Analytical biochemistry*, 1994, **218**, 1–13.
- 513 27 A. Mehranfar, K. Bordbar and R. Amiri, *Biomacromol. J.*, 2015, **1**, 69–79.

- 514 28 M. Ying, F.W. Huang, H. D. Ye, H. Xu, L. L. Shen, T. W. Huan, S. T. Huang, J. F. Xie, S.
515 L. Tian and Z. L. Hu, *Int. J. Biol. Macromol.*, 2015, **79**, 201-208.
- 516 29 F. Mohammadi and M. Moeeni. *Mater Sci Eng C Mater Biol Appl.*, 2015, **50**, 358-66.
- 517 30 J.L.Wang and G.M.Edelman, *J. Biol. Chem.*, 1971, **246**, 1185-1191.
- 518 31 S.Nöbel, K. Weidendorfer and J. Hinrichs, *J. Colloid Interface Sci.*, 2012, **386**, 174-80.
- 519 32 S. Y. Yazdi, M. Corredig and D. G. Dalgleish, *Food Hydrocoll.*, 2014, **42**, Part 1, 171–
520 177.
- 521 33 J. Phadungath, *J. Sci. Technol.*, 2005, **27**, 201-212.
- 522 34 D.G. Dalgleish, *Soft Matter*, 2011, **7**, 2265–2272.
- 523 35 S. Marchin, J.-L. Putaux, F. Pignon and J. Léonil, *J. Chem. Phys.*, 2007, **126**, 045101
- 524 36 C. G. De Kruif, *J. Appl. Crystallogr.*, 2014, **47**, 1479–1489
- 525 37 R. Chang, L. Sun and T. J. Webster, *Int. J. Nanomedicine*, 2014, **9**, 461–465
- 526 38 D. Z. Liu, M. G. Weeks, D. E. Dunstan and G. J.O. Martin, *Food Chemistry*, 2013,**141**,
527 4081–4086.
- 528 39 T. H. M. Snoeren, H. J. Klok, A. C. M. Van Hooydonk and A. J. Damman,
529 *Milchwissenschaft*, 1984, **39**, 461–463.
- 530 40 L. Zhao, S. Zhang, H. Uluko, L. Liu, J. Lu, H. Xue, F. Kong and J. Lv , *Food Chem.*,
531 *2014*, **165**, 167–174.
- 532 41 M. Bernabé-Pineda, M. T. Ramírez-Silva, M. Romero-Romo, E. González-Vergara and A.
533 Rojas-Hernández, *Spectrochim. Acta. A. Mol. Biomol. Spectrosc.*, 2004, **60**, 1091–1097.
- 534
- 535

536

537

538

539

540

Table 1: Values of the Stern-Volmer constant K_{sv} , the binding constant K_b , and the number of protein sites n , for curcumin-MC mixtures at different pH values. Experiments were made in triplicate at 25 °C.

pH	K_{sv} ($\times 10^4$ M ⁻¹)	K_b ($\times 10^4$ M ⁻¹)	n
7.4	18.8 ± 0.9	3.9 ± 0.4	1.47 ± 0.02
6.5	18.2 ± 0.2	7.8 ± 1.3	1.25 ± 0.06
6.0	21.9 ± 0.5	9.2 ± 1.6	1.25 ± 0.05
5.5	24.1 ± 1.5	7.7 ± 1.2	1.38 ± 0.06
5.0	32.5 ± 1.5	7.5 ± 0.7	1.49 ± 0.05

541

542

543

544 Table 2: Variation of K_b values (eq. 3) as a function of temperature. Experiments were made in
545 triplicate.

Temperature(°C)	K_b ($\times 10^4 M^{-1}$)
20	0.6 ± 0.3
25	2.2 ± 0.5
30	3.8 ± 1.2
35	6.6 ± 0.6

546
547

Figures captions

Figure 1. Fluorescence emission induced by the binding of curcumin to casein micelles. (A) Intrinsic fluorescence emission spectra of 8.9 μM casein micelles in the presence of increasing concentrations of curcumin (0 - 50 μM , a-j curves). Excitation wavelength (λ_{exc}) was set at 280 nm. (B) Intrinsic fluorescence emission spectra of 5 μM curcumin ($\lambda_{\text{exc}} = 420$ nm) at increasing concentrations of casein micelles (0 - 55.8 μM , a-k curves). (C) Fluorescence quenching of 8.9 μM casein micelles at $\lambda_{\text{em}} = 344$ nm ($\lambda_{\text{exc}} = 280$ nm) with increasing curcumin concentration (0 - 40 μM). (D) Fluorescence intensity of curcumin at $\lambda_{\text{em}} = 500$ nm ($\lambda_{\text{exc}} = 280$ nm) with increasing concentrations of casein micelles (0 - 55.8 μM). (E) Double logarithmic plot: $(F_0 - F)/F$ vs. [curcumin] from fluorescence quenching experiments. (F) Double reciprocal plot: $1/(F - F_0)$ vs. $1/[\text{casein micelles}]$ from fluorescence intensity experiments.

Figures 2. (A) Normalized fluorescence intensity of 5 μM curcumin at 500 nm ($\lambda_{\text{exc}} = 420$ nm) in the presence of increasing casein micelles concentrations (0, 5.6, 11.2, 13.9, 16.7, 19.5, 22.3, 27.9, 33.5, 39, 44.6, 50.2, and 55.8 μM) at 20, 25, 30, 35, and 40 $^{\circ}\text{C}$ ($n = 3$). (B) Casein micelles concentrations at half maximal fluorescence in the 20 - 40 $^{\circ}\text{C}$ temperature range.

Figure 3. Small Angles X-Ray Scattering profiles of casein micelles dispersions. Circles and diamonds: 6.7 μM CM in the absence of curcumin respectively recorded at long and short sample-detector distances; squares, triangles, and orange triangles: 6.7 μM casein micelles and 1.5, 2.3, and 4.6 μM curcumin, respectively, recorded only at long sample-detector distance. (A) superimposed curves and (B) curves shifted for clarity purposes.

Figure 4. Fluorescence quenching of casein micelles (8.9 μM) after MC acidification overnight by hydrolysis of GDL at pH values from 7.5 to 5.0. $\lambda_{\text{em}} = 344$ nm ($\lambda_{\text{exc}} = 280$ nm) with increasing concentrations of curcumin (0 - 30 μM) at 25 $^{\circ}\text{C}$. Represented values are the mean of three replicates. Dotted lines correspond to kinetic induced by hydrolysis of GDL in MC suspension containing 0 and 20 μM curcumin. The fluorescence offset between pH stabilized and kinetic experiments performed with curcumin concentration of 0 and 20 μM is due to different apparatus configurations.

Figure 5. Backscattered intensity measurements on MC-curcumin sample at 35 $^{\circ}\text{C}$: (A) Evolution of the relative percentage of backscattered intensity (ΔBS) ($t_0 = \text{reference}$) upon sample height after GDL addition during 115 min (one scan every 5 minutes). (B) Evolution of the ΔBS average (calculated from sample height between 15 and 45 mm) and elastic modulus (G') upon time after GDL addition.

Figure 6. Evolution of (A) the elastic modulus and of (B) the relative percentage of backscattered intensity upon GDL acidification of MC and MC-curcumin samples at 20 and 35 $^{\circ}\text{C}$.

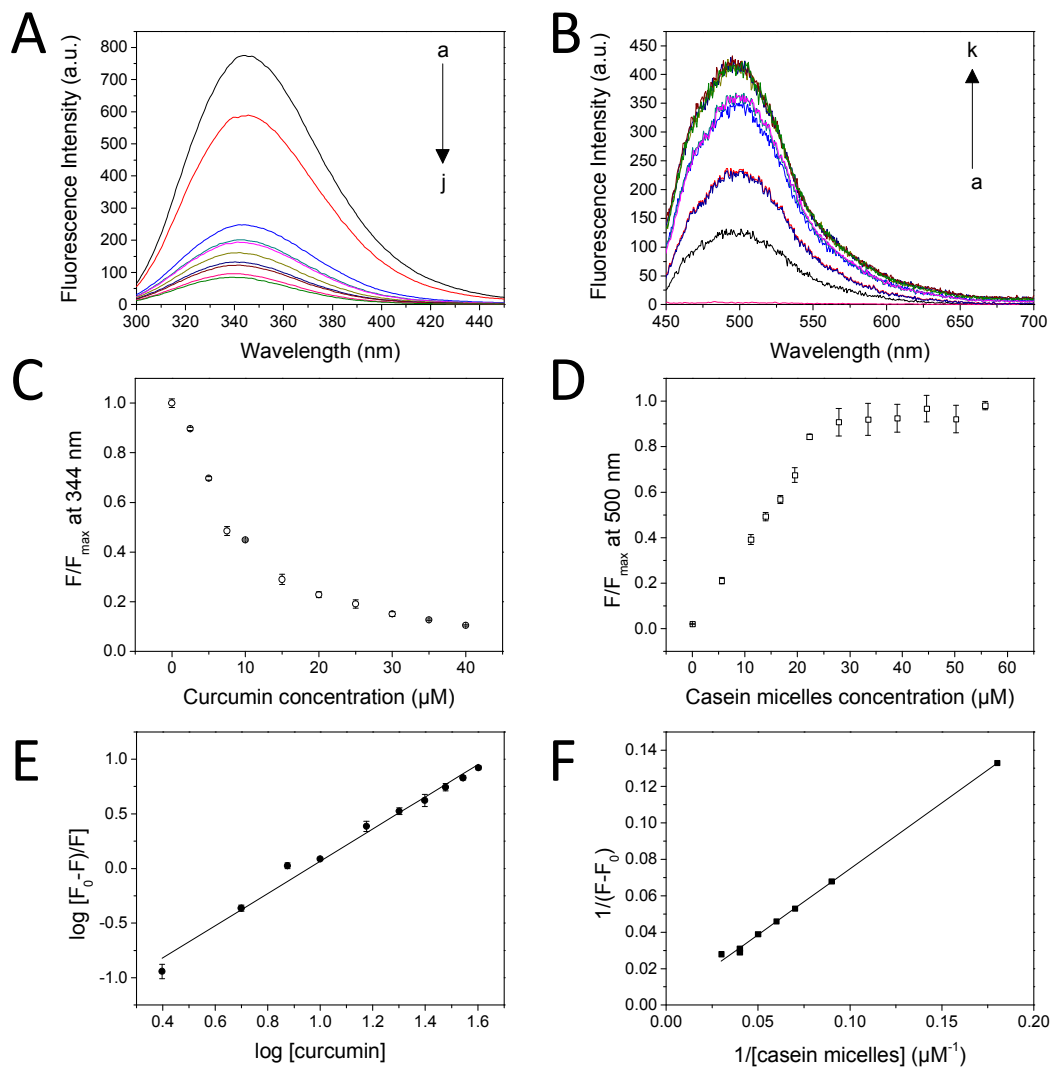


Figure 1

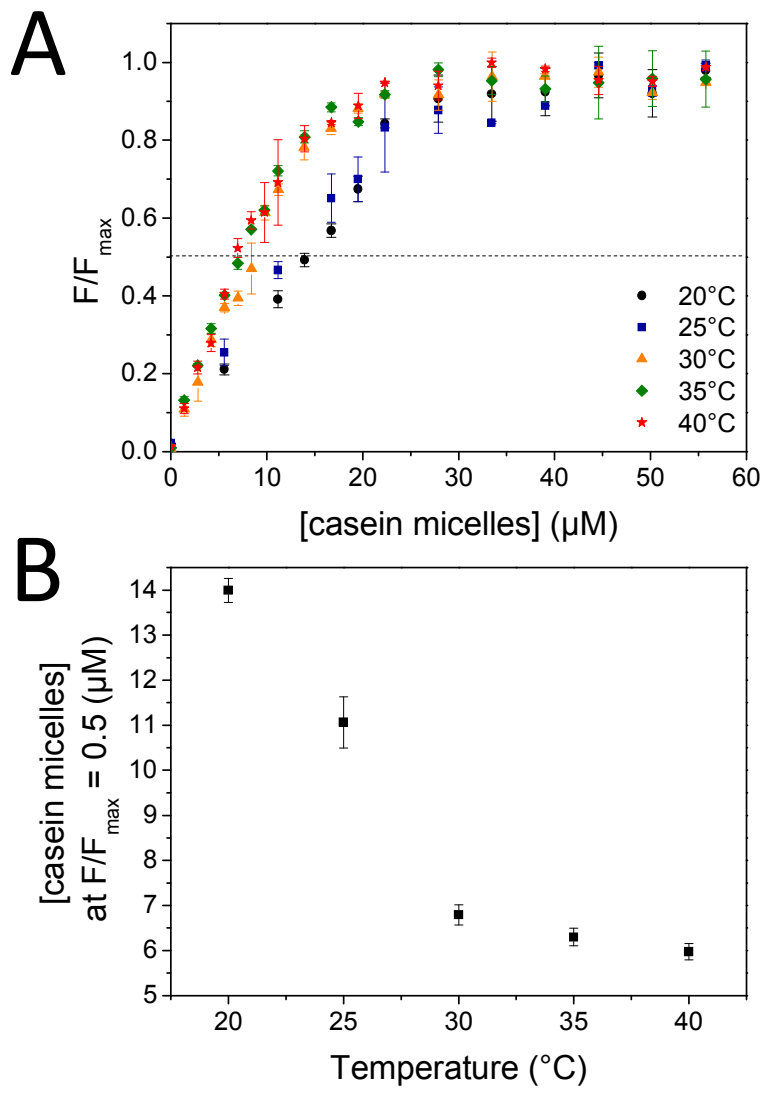


Figure 2

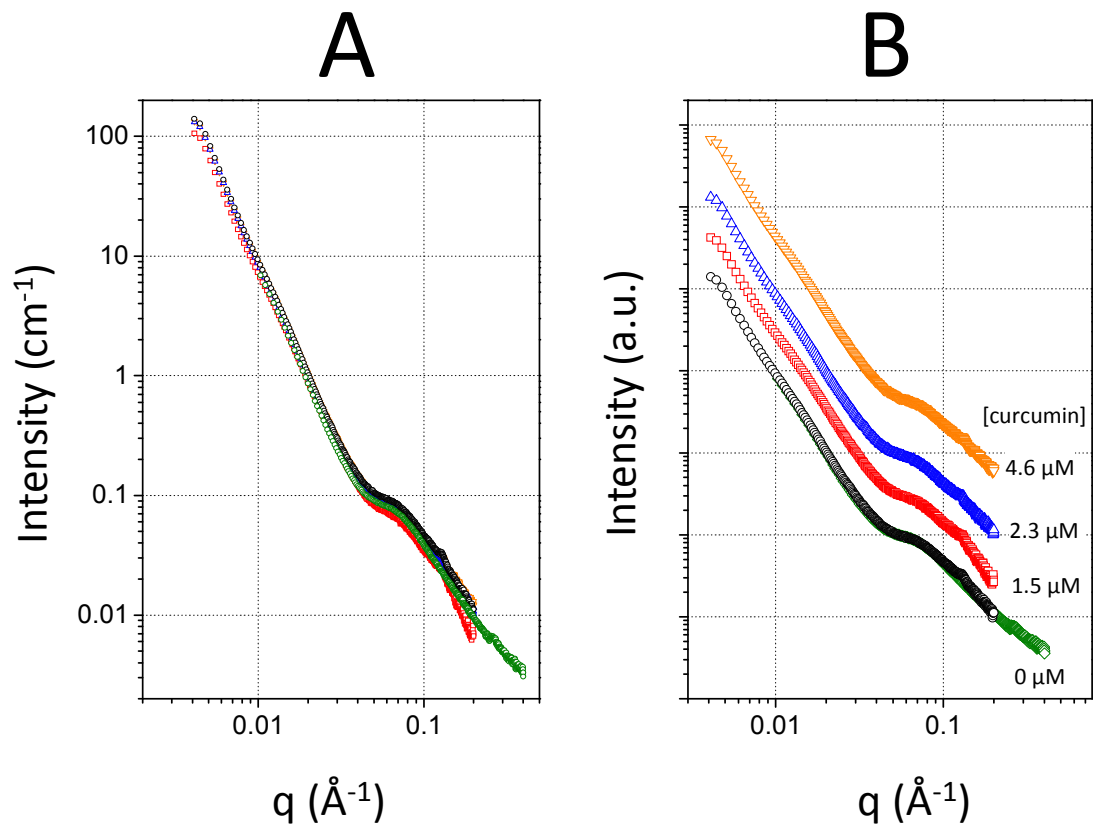


figure 3

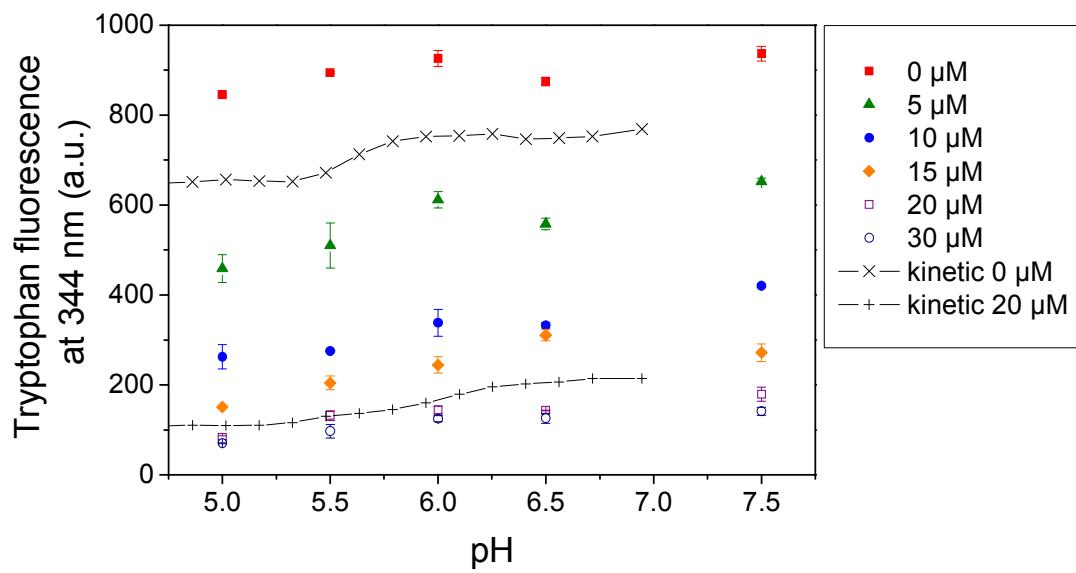


figure 4

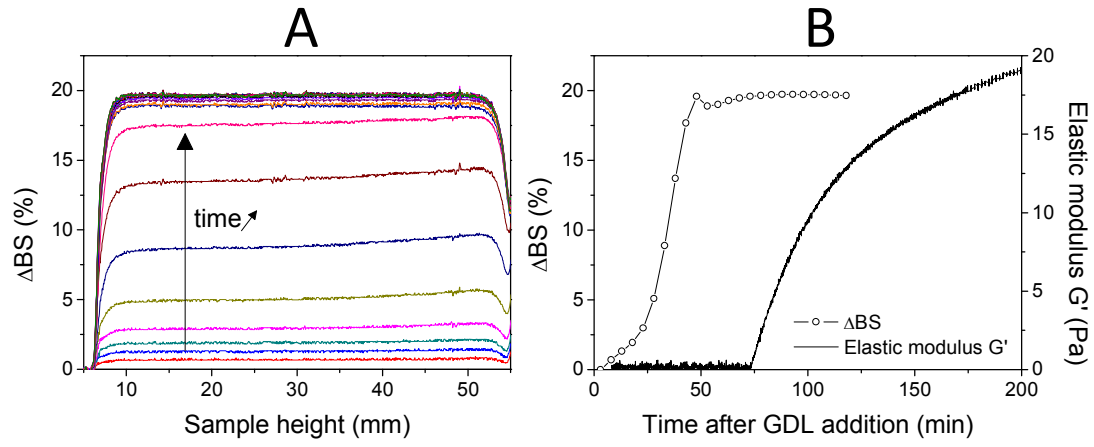


Figure 5

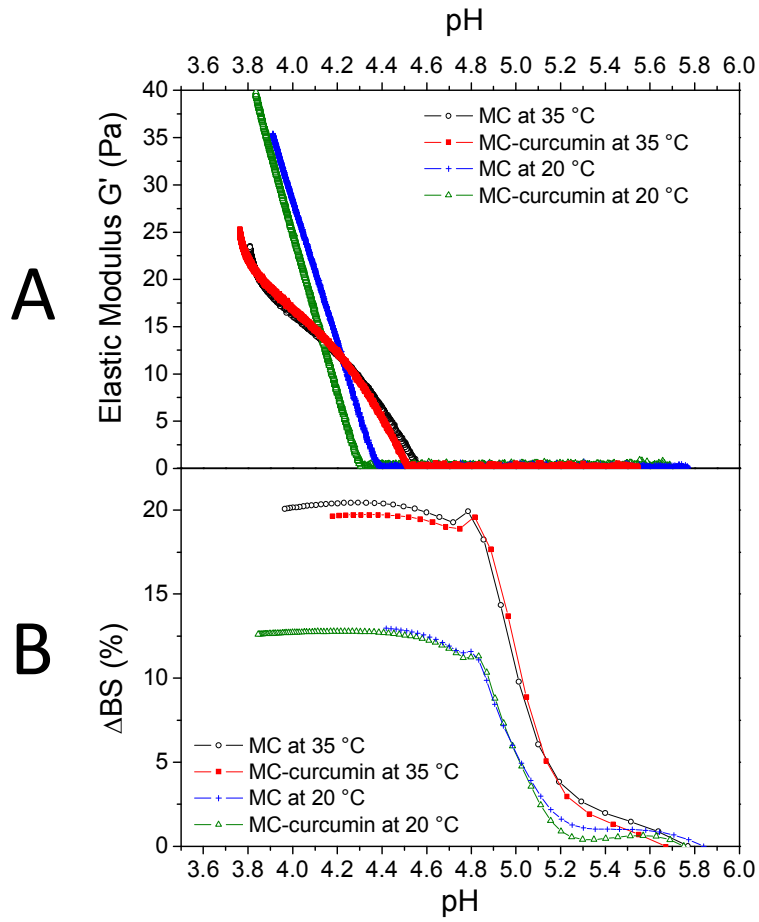


Figure 6

